TECHNICAL NOTE

Magnetic Resonance in Medicine

Three-dimensional gradient and spin-echo readout for time-encoded pseudo-continuous arterial spin labeling: Influence of segmentation factor and flow compensation

Andre M. Paschoal[1,2,3,4] | **Renata F. Leoni**[2] | **Bruno F. Pastorello**[3] | **Matthias J. P. van Osch**[4]

[1]Medical School of Ribeirao Preto, University of Sao Paulo, Ribeirao Preto, SP, Brazil

[2]InBrain Lab, Department of Physics - FFCLRP, University of Sao Paulo, Ribeirao Preto, SP, Brazil

[3]LIM44 - Instituto e Departamento de Radiologia, Faculdade de Medicina - Universidade de São Paulo, São Paulo, SP, Brazil

[4]C.J. Gorter Center for High Field MRI, Department of Radiology, Leiden University Medical Center, Leiden, The Netherlands

Correspondence
Andre M. Paschoal, LIM44, Instituto e Departamento de Radiologia, Faculdade de Medicina, Universidade de São Paulo, São Paulo, SP 05403-010, Brazil.
Email: andre.paschoal@usp.br

Twitter: @paschoal_am

Purpose: To monitor the complete passage of the labeled blood through the vascular tree into tissue and improve the quantification of ASL maps, we evaluated the effect of 3D gradient and spin-echo (GRASE) readout segments on temporal SNR (tSNR) and image blurriness for time-encoded pseudo-continuous arterial spin labeling and the effect of flow-compensation gradients on the presence of intravascular signal.

Methods: Fifteen volunteers were scanned using time-encoded pCASL with 2D EPI and single-segment, two-segments, and three-segments 3D-GRASE readouts with first-order flow compensation (FC) gradients. Two-segments 3D-GRASE scans were acquired with 25%, 50%, 75%, and 100% of full first-order FC. Temporal SNR was assessed, and cerebral blood flow and arterial blood volume were quantified for all readout strategies.

Results: For single-segment 3D GRASE, tSNR was comparable to 2D EPI for perfusion signal but worse for the arterial signal. Two-segments and three-segments 3D GRASE resulted in higher tSNR than 2D EPI for perfusion and arterial signal. The arterial signal was not well visualized for 3D-GRASE data without FC. Visualization of the intravascular signal at postlabeling delays of 660 ms and 1060 ms was restored with FC. Adequate visualization of the intravascular signal was achieved from 75% of FC gradient strength at a postlabeling delay of 660 ms. For a postlabeling delay of 1060 ms, full-FC gradients were the best option to depict intravascular signal.

Conclusion: Segmented GRASE provided higher effective tSNR compared with 2D-EPI and single-segment GRASE. Flow compensation with GRASE readout should be carefully controlled when applying for time-encoded pCASL to visualize intravascular signal.

1 | INTRODUCTION

Arterial spin labeling (ASL) is a noninvasive perfusion-weighted imaging technique that exploits arterial blood as an endogenous tracer. A bolus of arterial blood is magnetically labeled through inversion in a slab proximal to the imaging plane, from which it will flow through the arterial tree until crossing the blood-brain barrier and reaching the brain-tissue compartment. After labeling the blood through the application of RF pulses has stopped, the image is acquired after a time interval called postlabeling delay (PLD). A single PLD is considered adequate to measure cerebral blood flow (CBF).[1] However, when the subject suffers from prolonged arterial transit time (ATT), CBF will be underestimated, which can be corrected by acquiring a multiple-timepoint ASL (multi-PLD ASL).

Moreover, multi-PLD ASL allows monitoring the labeled arterial blood within the intravascular space at short PLDs, until finally perfusing the brain tissue at the later PLDs. By using, for example, Bayesian inference under the appropriate kinetic model, all PLDs are used to estimate quantitative ASL maps, which include the CBF, arterial blood volume (aBV), and ATT. In such a model, all PLDs acquired are important for the final CBF maps to be corrected for arrival-time artifacts and intravascular signal.

In 2015, a consensus paper set the recommended implementation of ASL for clinical applications,[1] to help with standardization and dissemination of the technique. In summary, a segmented 3D gradient and spin-echo (GRASE) readout[2-4] was recommended in combination with pseudo-continuous arterial spin labeling (pCASL), as it can be optimally combined with background suppression using a single excitation pulse per TR, resulting in higher SNR compared with 2D EPI.[5,6] However, choosing the number of segments for 3D GRASE requires fine-tuning to balance SNR, blurring in z-direction, and vulnerability to motion. Segmented 3D sequences fill less k-space lines per excitation pulse, thereby reducing signal losses due to T_2^* and consequently providing less blurring at boundaries between tissues, especially where a significant signal difference exists (eg, between CSF and gray matter). Therefore, segmented acquisitions are less suited in situations in which many different conditions need to be measured, such as in multi-postlabeling delays (PLD) ASL. Although single-segment 3D GRASE provides a more time-efficient acquisition, it results in significant blurring in z-direction, so it has been scarcely used.

There are three main approaches for multi-PLD ASL. First, traditional pCASL scans can be repeated with different PLDs and labeling duration. Recently, Woods et al[7] proposed optimal settings for such an acquisition. Second,

a Look-Locker readout can be used as, for example, in the inflow turbo-sampling EPI–flow-sensitive alternating inversion recovery and QUASAR (Modus QA, London, ON, Canada) sequences.[8,9] This approach has the advantage that all PLDs are acquired simultaneously, albeit with lower SNR resulting in similar total scan times. Finally, Hadamard-encoded pCASL or time-encoded pCASL (te-pCASL) was demonstrated, which achieves multiple PLDs by the temporal encoding of the labeled blood following a Hadamard matrix.[10-13] When designing a 3D readout sequence for multi-PLD acquisitions, the criteria are different compared with single-PLD perfusion imaging. Special attention is needed when considering the use of flow compensation (FC) gradients that compensate for first-order dephasing effects.[14] Use of FC can increase TE and readout times, but its absence will crush vascular ASL signal, which is an essential part of the information conveyed in early PLDs by showing the passage of label through the arterial system.

The appropriate readout setup and use of FC gradients provide the promise of images with higher temporal SNR (tSNR) and improved delineation of the angiographic phase, respectively, as an input for the quantitative model, which would lead to more accurate CBF, aBV, and ATT maps. Therefore, we aimed to evaluate the effect of the number of segments of 3D-GRASE readout on tSNR, comparing its performance with the 2D-EPI readout, and analyze the effect of FC gradients in delineating the presence of vascular signal.

2 | METHODS

2.1 | Hadamard-encoded pCASL

Time-encoded pCASL is a time-efficient strategy to acquire multi-PLD pCASL, providing the opportunity to monitor the dynamic inflow of blood into brain tissue, improving CBF quantification, and allowing the measurements of ATT and aBV. In a time-encoded acquisition, the labeling module is divided into small subboli, encoded according to a Hadamard matrix to be either control or label. In this study, a Hadamard-8 matrix was chosen for the labeling module, with a total labeling duration of 3500 ms split into seven blocks of 1800, 800, 400, 2×150, and 2×100 ms (ie, the free-lunch approach).[13] After the labeling module, there was a PLD of 160 ms until starting the readout module (Figure 1B). Two background suppression pulses were applied at 1831 ms and 3135 ms.
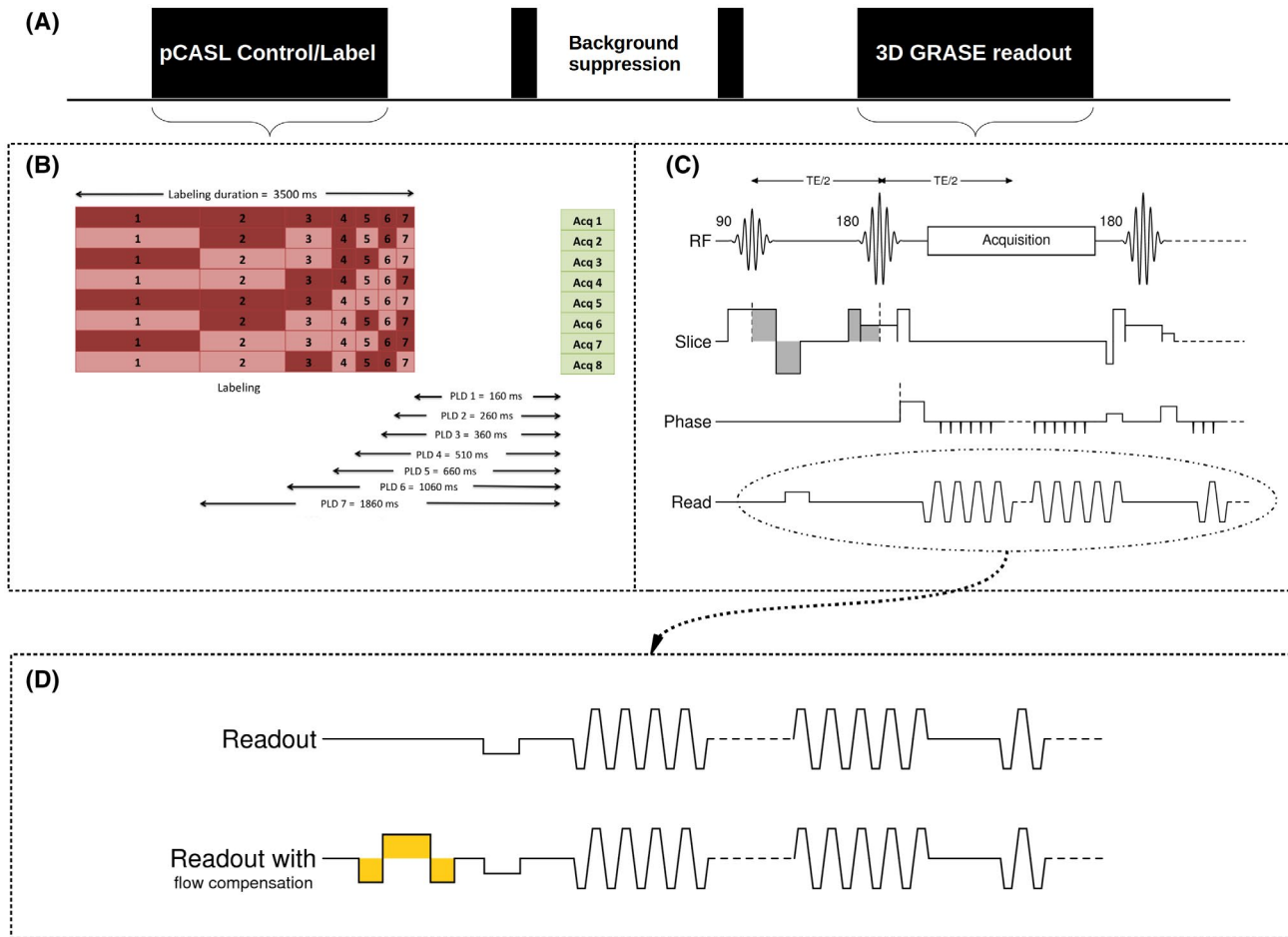
FIGURE 1 A, Pulse sequence diagram of 3D time-encoded pseudo-continuous arterial spin labeling (te-pCASL). B, Eight Hadamard matrix for pCASL labeling encoding, followed by the even postlabeling delay (PLD) intervals (in which the background suppression pulses are applied) until reaching the readout module for acquisitions 1 to 8. C, Three-dimensional gradient and spin-echo (GRASE) readout module. When the image is acquired with a single segment, the whole-brain acquisition is achieved with only one 90° RF excitation pulse, whereas for two-segments and three-segments images, the readout module is repeated two and three times, respectively, (two and three 90° RF excitation pulses) to acquire a whole-brain volume. D, When flow compensation is desired, bipolar gradient lobes are applied in the readout direction just before the acquisition

2.2 | Three-dimensional GRASE readout: Number of segments

The 3D-GRASE readout combines the time efficiency of EPI with higher SNR of 3D imaging by exploiting the rapid imaging with refocused echoes readout[15] technique in the z-direction (Figure 1C). When an entire volume is acquired using only a single excitation pulse, the approach is called single-segment 3D GRASE. When more than one segment is required to fill the 3D k-space, the approach is referred to as multisegmented or segmented 3D GRASE. Because T_2 signal decreases over the readout train result in blurring on the kz-axis, GRASE segmentation is recommended. In this study, we evaluated how the number of segments in 3D-GRASE readout influences the te-pCASL acquisition performance concerning time efficiency, blurring in the z-direction, and SNR. Moreover, the results were compared with a 2D multislice EPI readout.

2.3 | Three-dimensional GRASE readout: FC

The purpose of using FC gradients is to correct for flow-induced dephasing. It can be achieved using additional bipolar gradient lobes before the signal readout (Figure 1D). As the area under the positive and negative lobes are the same, the added mean gradient is zero, but the timing of each gradient lobe is chosen, so that the spins flowing with constant velocity end up with zero phase accumulation over the total readout (ie, no dephasing). For first-order FC, the dephasing is only circumvented for constant velocity (ie, acceleration [deceleration] of blood can still lead to dephasing). Due to the added gradients, flow compensation will increase TE value and lengthen the total readout time. Nonetheless, especially when using a 3D readout, visualization of intravascular signal of dynamic ASL signal can be considered critical, especially during the inflow phase. Therefore, we analyzed the

effect of FC gradients scaling for two-segments 3D-GRASE readout on the resulting images, for both the angiographic and the perfusion phase of multi-PLD time-encoded ASL.

2.4 | Magnetic resonance imaging experiments details

Fifteen volunteers (8 females, age 26.3 ± 5.2 years) were scanned on a 3T Philips MRI scanner (Amsterdam, Netherlands), from which 10 were scanned for the readout segmentation experiment and five for the FC experiment. All volunteers agreed to participate after signing informed consent, and the study was in agreement with local internal review board policies. We used a time-encoded Hadamard-8 pCASL labeling sequence with single-segment, two-segments, and three-segments 3D GRASE and a multislice 2D-EPI readout. Table 1 lists the acquisition parameters.

For the FC experiment, two-segments 3D-GRASE scans were acquired with the FC gradient strengths of 0%, 25%, 50%, 75%, and 100% of full first-order strength to analyze the effect of FC on the visualization of the vascular ASL signal.

2.5 | Data analysis

Hadamard matrix decoding for ASL subtraction was performed in *MATLAB* (MathWorks, Natick, MA) to obtain multi-PLD ASL maps (note that labeling duration is also different among the multi-PLD maps). Further processing of

ASL data and quantification of CBF and aBV were performed using the BASIL toolkit (Oxford Center for Functional MRI of the Brain's software library [FSL]),[16,17] considering all PLDs acquired. Scans were corrected for motion using the MCFLIRT tool (FSL), and the structural images were segmented and transformed into the ASL space to create whole-brain, gray-matter, and white-matter masks using FAST and FLIRT tools (FSL).

Perfusion images were deblurred using the oxasl-deblur toolkit of the Quantitative Biomedical Inference Group, Oxford Institute of Biomedical Engineering (https://oxasl.readthedocs.io/en/latest/download.html), which uses a fast Fourier transform filter in the frequency space to reduce the blurring in z-direction for 3D-GRASE data. Furthermore, both blurred and deblurred ASL perfusion maps were compared with the gray-matter region of interest of the T_1-weighted structural images transformed to the ASL space (reference image). The blurring estimation in z-direction was done in *MATLAB* using a method that compares the desired image with a reference image and outputs the blurring of the input image.[18]

Postprocessing and calculation of tSNR was done in *MATLAB* according to:

$$tSNR = \frac{S}{\sigma} * \sqrt{\frac{\text{Number of averages in 6 min}}{\text{Total averages acquired}}}, \quad (1)$$

where S is the mean signal of a voxel over the different averages, and σ is the SD. The perfusion tSNR was voxel-wise calculated within the region of interest of the gray-matter mask

TABLE 1 Acquisition parameters

Scan parameter	2D EPI	3D GRASE Single segment	3D GRASE Two segments	3D GRASE Three segments
FOV (mm)	240 × 240	240 × 240 × 102	240 × 240 × 102	240 × 240 × 102
Voxel size (mm)	3.75 × 3.75 × 6	3.75 × 3.75 × 6	3.75 × 3.75 × 6	3.75 × 3.75 × 6
Acquisition matrix	64 × 64 × 17	64 × 64 × 31	64 × 64 × 31	64 × 64 × 31
Reconstructed slices	17	17	17	17
Oversampling factor	–	1.8	1.8	1.8
Slice thickness (mm)	6	6	6	6
TR (ms)	4100	4100	3900	3900
TE (ms)	9.2	9.2	13.9	10.5
No. of repetitions	6	6	3	2
EPI factor	25	25	13	5
TSE factor	–	16	16	16
Bandwidth (Hz) (frequency direction)	3136	3160	3160	3160
SENSE factor (AP direction)	2.5	2.5	2.5	2.5
Total scan duration (minutes)	6:03	6:15	7:56	12:10
FC	No	Yes	Yes	Yes

Abbreviations: AP, anterior–posterior; TSE, turbo spin echo.
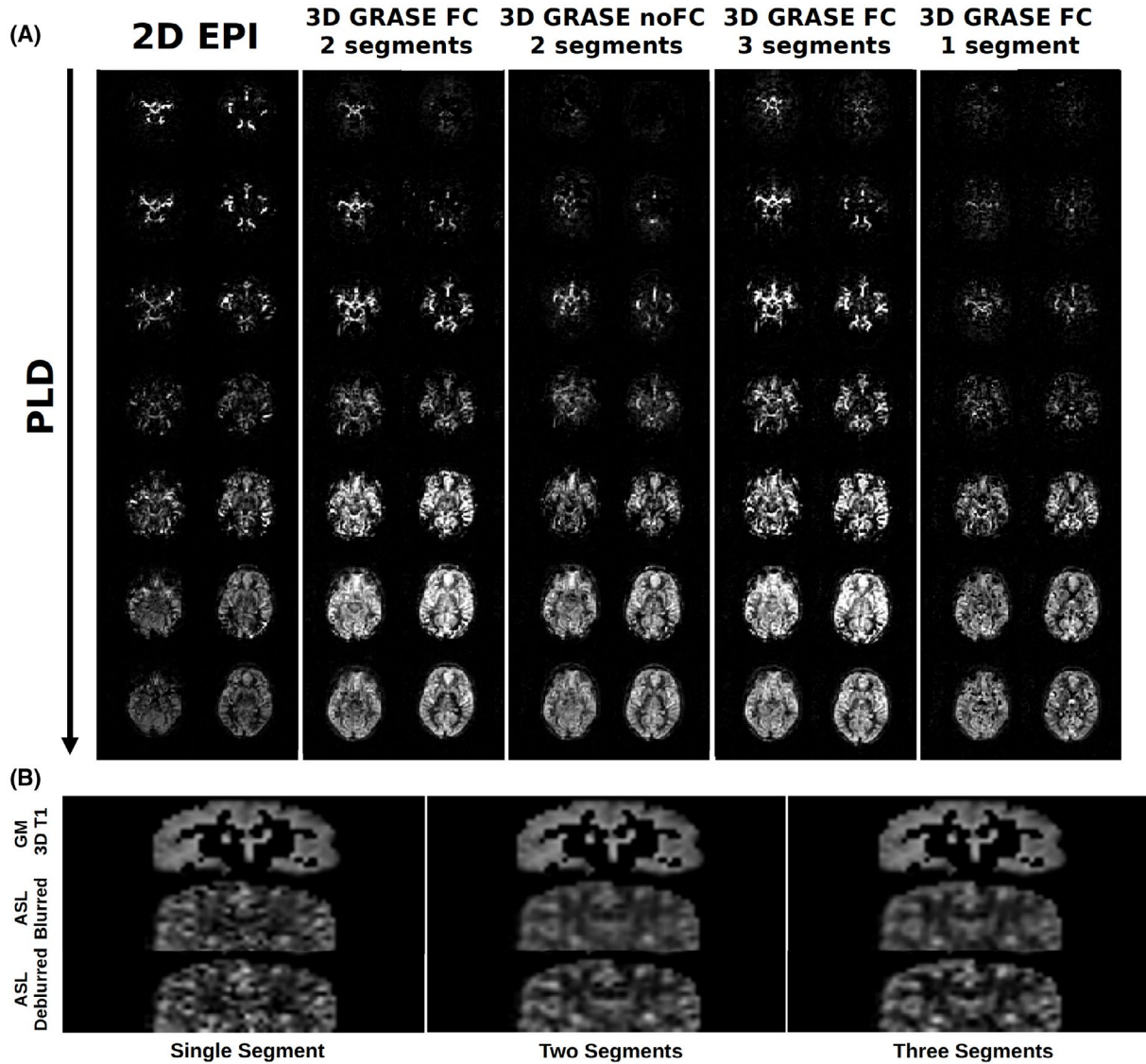
FIGURE 2 A, Two representative slices for all PLDs and readout schemes. B, Comparison of gray matter (GM) of 3D T_1 images transformed to ASL space with blurred and deblurred ASL images for each of the 3D-GRASE readouts acquired. Abbreviation: FC, flow compensation

transformed to the ASL images space, whereas for the vascular tSNR analysis, we used the aBV outputs from the two-segments 3D GRASE thresholded at 1 mL/100 g/min. The contrast-to-noise ratio (CNR) was calculated for the perfusion block (PLD of 1860 ms) for all readouts, according to:

$$CNR = \frac{mean\,(GM) - mean\,(WM)}{\sigma_s}, \quad (2)$$

where mean(GM) and mean(WM) are the mean signal over the gray-matter and white-matter masks, and σ_s is the spatial SD of the whole-brain ASL images.

The statistical analysis was performed in R.[19] A one-way ANOVA was used to compare tSNR among different numbers of segments and FC levels. We also performed the two-way ANOVA to compare CNR and blurring levels. In such cases, the factors were the number of segments and the use or not of deblurring. Results were adjusted for multiple comparisons using the Tukey's method.

3 | RESULTS

3.1 | Effects of segmentation number

Two representative slices of ASL maps at multiple PLDs are shown in Figure 2A for axial view and in Supporting Information Figure S1 for sagittal views for the 3D-GRASE readout with different numbers of segments and the 2D multislice scan. The sagittal maps are shown to assess blurring in z-direction, which is especially apparent in the single-segment GRASE scan. Figure 3 shows the tSNR maps in axial directions for two representative PLDs that focus on the intravascular (left) and the perfusion signal (right panel). For
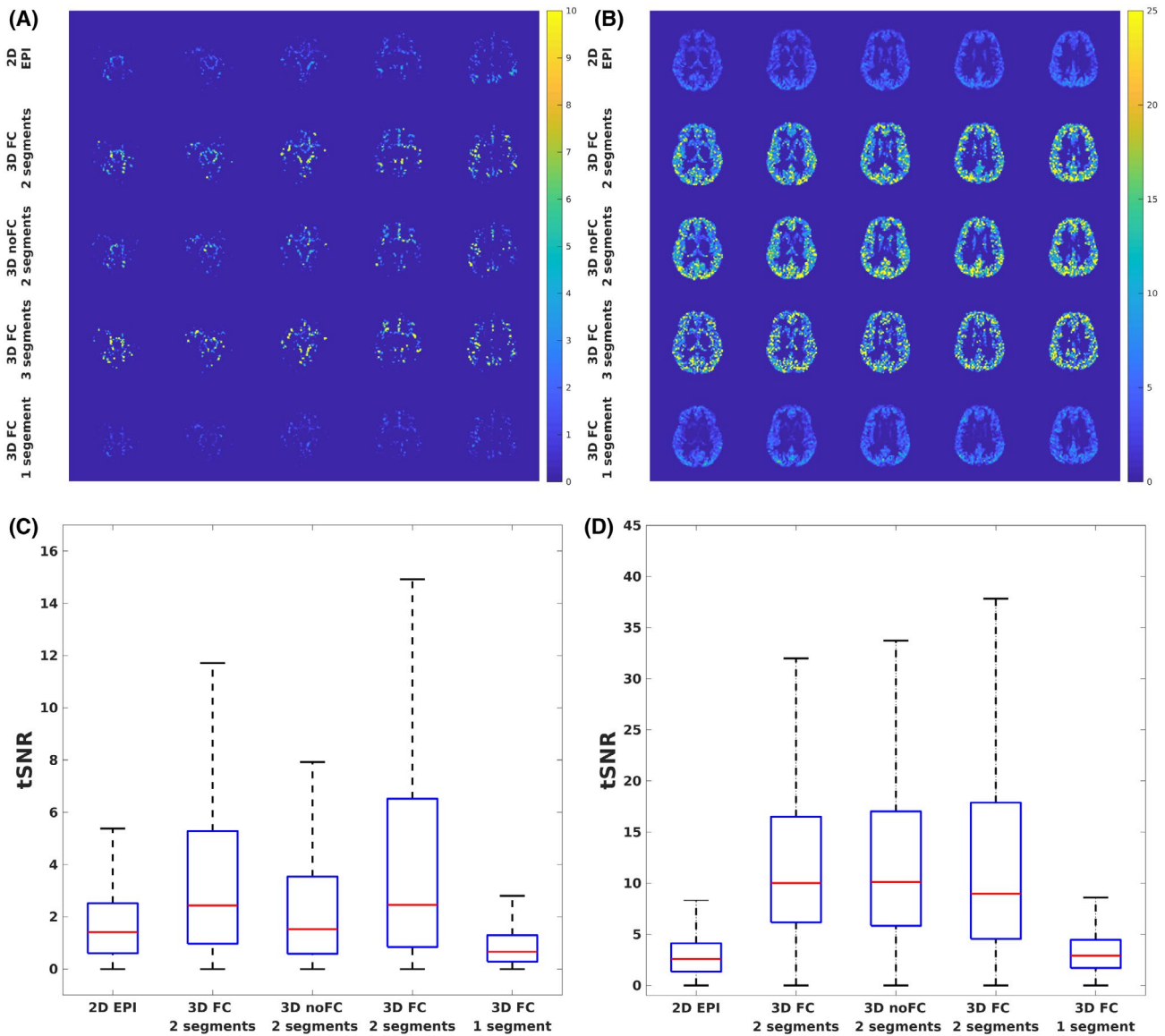
FIGURE 3 Temporal SNR (tSNR) calculated for all readouts at a PLD of 660 ms (A,C) and 1860 ms (B,D)

the PLD of 660 ms, the EPI readout had significantly higher tSNR (0.85 ± 1.01, $P < .01$) than the single-segment 3D GRASE (0.54 ± 0.60), whereas the tSNR for both the two-segments and three-segments 3D GRASE (tSNR = 2.17 ± 3.90 and 3.10 ± 7.39, respectively), were significantly higher than the single-segment 3D GRASE and the 2D-EPI readout ($P < .01$). For the perfusion signal measured at a PLD of 1860 ms, all 3D-GRASE acquisitions showed higher tSNR than the 2D-EPI readout (tSNR = 2.94 ± 2.12, $P < .01$), and the two-segments and three-segments 3D GRASE (tSNR = 13.60 ± 12.55 and 14.88 ± 17.12, respectively) exhibited significantly higher tSNR than single-segment 3D GRASE (tSNR = 3.33 ± 2.33, $P < .01$).

The comparisons between blurred and deblurred images for single, two, and three segments are shown in Figure 2B (coronal view). The comparison between the two-segments

and three-segments images did not show significant differences (blurring = $42.20 \pm 5.42\%$ vs $34.86 \pm 7.46\%$, $P > .05$) for blurred images. For deblurred images, the three-segments images showed significantly lower blurring (blurring = $5.19 \pm 4.20\%$, $P < .05$) than the two-segments ($11.82 \pm 8.47\%$) and single-segment images ($10.09 \pm 4.97\%$). The CNR measurements revealed significantly higher values ($P < .01$) for two-segments and three-segments 3D GRASE (CNR = 0.32 ± 0.03 and 0.33 ± 0.02, respectively), compared with single-segment 3D GRASE (0.201 ± 0.037) and 2D EPI (0.204 ± 0.023).

For a better analysis of the vascular signal, aBV maps were calculated from the multi-PLD images for different numbers of segments (see Supporting Information Figure S2A). The CBF maps were also quantified for different numbers of segments, taking all PLDs into account (see Supporting Information Figure S3A).
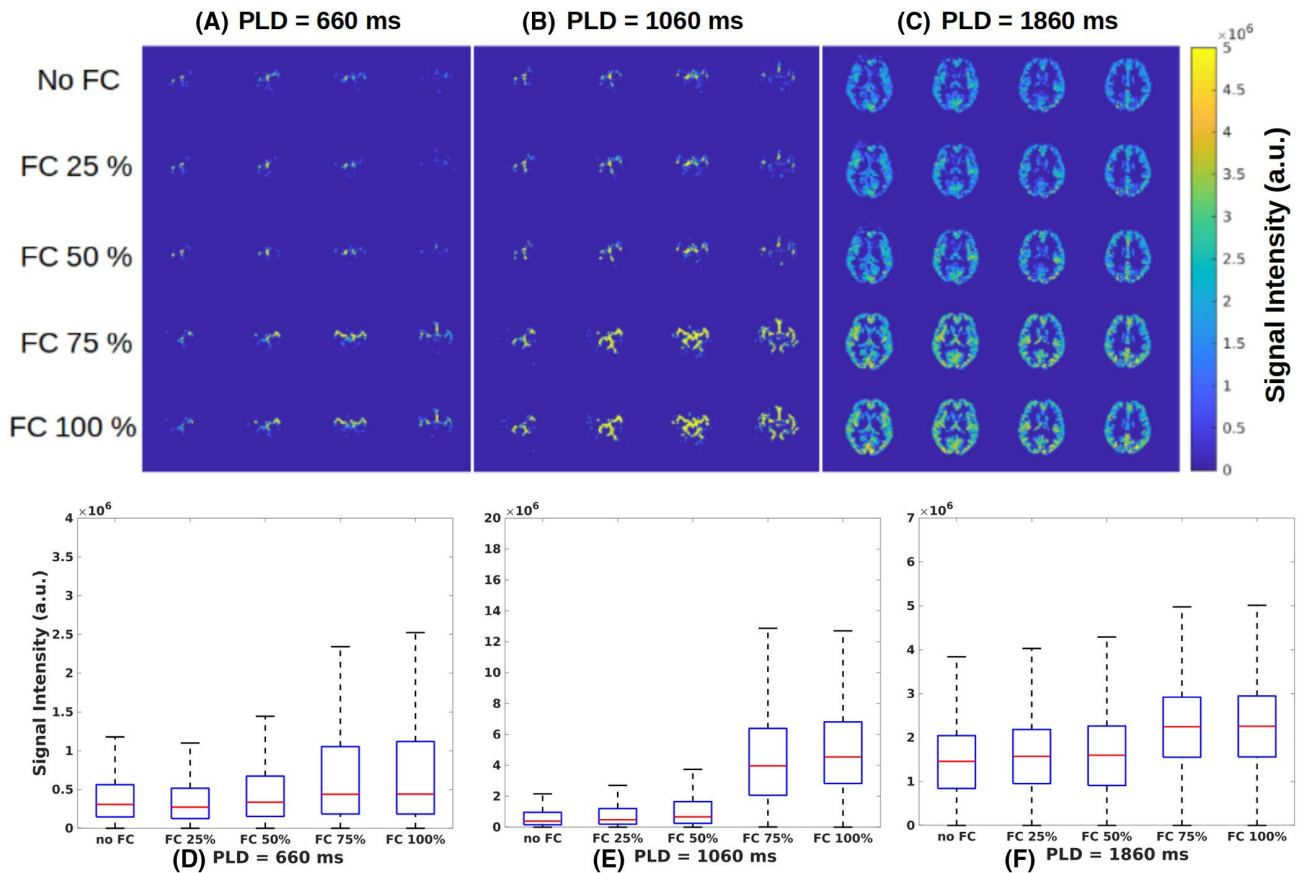
FIGURE 4 Signal intensity calculated for different levels of FC at a PLD of 660 ms (A,D), 1060 ms (B,E), and 1860 ms (C,F). For the PLD of 660 ms, the comparison between the FC of 25% and no FC and between FC of 50% and no FC did not show statistical difference ($P < .01$). For the PLD of 1060 ms, the only comparison that did not show statistical difference ($P < .01$) was between the FC of 25% and FC of 50%, whereas for the PLD of 1860 ms, the only comparison that did not result in significant difference was between FC of 75% and FC of 100%

3.2 | Effects of FC

Finally, the intensity of FC gradients was varied (Figure 1D), and the effect of the vascular signal on the visualization was evaluated. The FC gradient scaling was performed for two-segments 3D-GRASE te-pCASL, and the results are found in Supporting Information Figure S4 for two representative slices at multiple PLDs. The signal intensity maps for three representative PLDs are shown in Figure 4. We compared the signal intensities for different FC scales two by two. All comparisons were significant for a PLD of 660 ms ($P < .01$) except for no FC versus FC of 25%, and FC of 75% versus FC of 100%. No significant differences were observed between FC of 25% and FC of 50% for a PLD of 1060 ms, and between FC of 75% and FC of 100% for a PLD of 1860 ms. Finally, aBV and CBF maps from the respective FC scaling are shown in Supporting Information Figures S3B and S4B, respectively.

4 | DISCUSSION

In this study, the number of segmentations in 3D-GRASE readout and the use of FC gradients were evaluated for

te-pCASL. Optimal settings of 3D-GRASE readout for traditional pCASL imaging for perfusion measurements (ie, measured at a PLD of approximately 1.8 seconds) cannot be assumed optimal for te-pCASL due to two important differences: In te-pCASL, the angiographic phase of ASL is also captured, and the temporal footprint of te-pCASL (eight Hadamard encodings) is longer than for traditional pCASL (two conditions: label and control). The main findings of this study are 2-fold. First, segmented 3D GRASE outperforms single-segment 3D GRASE and multislice 2D EPI. Second, the use of proper FC is advised, to allow correct visualization of the angiographic phase.

The 2D-EPI readout showed good results for te-pCASL, allowing the visualization of both arterial and perfusion signal (Figure 2A). However, a more careful analysis revealed lower tSNR than segmented 3D GRASE (Figure 3). For perfusion signal, the tSNR of 2D EPI was lower than the one for single-segment 3D GRASE; for the angiographic phase, 2D EPI had a higher SNR than single-segment 3D GRASE. For two-segmented and three-segmented 3D-GRASE images, the tSNR values were significantly higher for both perfusion and arterial signal when compared with the 2D EPI (Figure 2A). When comparing the two-segments and three-segments 3D

GRASE, the latter produced the best results. Similar results were reported by Feinberg et al,[4] who analyzed the effects of the number of segments on single-PLD 3D-GRASE pulsed ASL data.

The blurring effects on 3D-GRASE data were also assessed. Previous studies reported a higher amount of blurring when using single-segment readout for 3D-GRASE ASL than a segmented acquisition.[4,20] However, they did not quantify the blurring, and the conclusion was based on visual inspection. We also observed a higher amount of blurring for single-segment 3D GRASE following visual inspection, but a quantitative analysis did not confirm this. This is probably because the tSNR and the spatial CNR are significantly lower than for segmented 3D GRASE. For segmented data, two-segments and three-segments images showed a comparable amount of blurring before applying a deblurring algorithm. After deblurring, the three-segments data were significantly less blurred than the two-segments 3D-GRASE images.

The aBV maps from data with first-order FC better delineated arterial signal. Similarly, two-segments and three-segments GRASE provided better aBV maps than single-segment GRASE (Supporting Information Figure S2A). As shown in the experiment in which the flow compensation was varied, FC use plays a big role in depicting the vascular signal.[21-24] The present results revealed that the intravascular signal visualization at PLDs of 660 ms and 1060 ms is hampered without FC (Figure 4A,B), with FC being especially essential at the PLD of 1060 ms (Figure 4B). At this PLD, and opposed to the PLD of 660 ms, most of the labeled blood already filled the large arteries within the imaging volume, while still flowing fast. For the even longer PLD of 1800 ms, the blood will have slowed down, resulting in a weaker influence of FC on image quality, although FC of 75% and 100% still provided slightly higher signal than lower FC levels. The smaller dependency on FC when the label arrives within the microvasculature and exchanges with tissue magnetization explains why FC has not been recognized earlier as an important sequence-design parameter. With the introduction of efficient multi-PLD ASL sequences, this effect becomes more prominent, as these sequences also focus on the more angiographic phase. The fact that still higher signal was observed with FC at a PLD of 1800 ms points to the fact that not all labels arrive at the capillary exchange site. Inclusion of a macrovascular component during postprocessing would correct for the label that did not arrive yet at the voxel of their final destination, similar to what Chappell et al has shown in a macrovascular component that still identifies a vascular signal in vascular crushed ASL data.[25] When the label would already have arrived in the final destination voxel, the signal should be included in quantification to provide the best estimate of perfusion.

The main limitation of this study is the investigation of FC gradients only in the readout direction. Future studies may explore their application in other directions. Another limitation is that we did not analyze the influence of motion, as segmented 3D GRASE results in a longer temporal footprint, making the acquisition more prone to motion artifacts.

5 | CONCLUSIONS

This study showed higher effective tSNR and CNR for two-segments and three-segments GRASE compared with 2D EPI and single-segment GRASE. Therefore, its use is recommended for te-pCASL. Moreover, FC properties of the GRASE readout should be carefully controlled when applying it to te-pCASL. The use of full FC is essential to visualize the inflow of blood through the arterial system, whereas without FC the vascular signal can be considerably dephased, hampering the assessment of the passage of the blood from the intravascular space to the brain tissue. With the complete passage, data modeling can be considered optimal, providing more accurate CBF, aBV, and ATT maps. When a single-segment readout is required, 3D GRASE and multislice EPI provide similar results regarding tSNR, although the tSNR for 2D EPI is higher for the angiographic phase.

ORCID
Andre M. Paschoal https://orcid.org/0000-0001-8269-711X
Renata F. Leoni https://orcid.org/0000-0002-4568-0746
Matthias J. P. van Osch https://orcid.org/0000-0001-7034-8959

REFERENCES
1. Alsop DC, Detre JA, Golay X, et al. Recommended implementation of arterial spin-labeled perfusion MRI for clinical applications: a consensus of the ISMRM perfusion study group and the European consortium for ASL in dementia. *Magn Reson Med.* 2015;73:102-116.
2. Oshio K, Feinberg DA. GRASE (gradient-and spin-echo) imaging: a novel fast MRI technique. *Magn Reson Med.* 1991;20:344-349.
3. Gunther M, Oshio K, Feinberg DA. Single-shot 3D imaging techniques improve arterial spin labeling perfusion measurements. *Magn Reson Med.* 2005;54:491-498.
4. Feinberg D, Ramann S, Gunther M. Evaluation of new ASL 3D GRASE sequences using parallel imaging, segmented and interleaved k-space at 3T with 12- and 32-channel coils. In: Proceedings of the 17th Annual Meeting of ISMRM, Honolulu, Hawaii, 2009. Abstract #622.
5. Ye FQ, Frank JA, Weinberger DR, McLaughlin AC. Noise reduction in 3D perfusion imaging by attenuating the static signal in arterial spin tagging (ASSIST). *Magn Reson Med.* 2000;44:92-100.

6. Garcia DM, Duhamel G, Alsop DC. Efficiency of inversion pulses for background suppressed arterial spin labeling. *Magn Reson Med*. 2005;54:366-372.

7. Woods JG, Chappell MA, Okell TW. A general framework for optimizing arterial spin labeling MRI experiments. *Magn Reson Med*. 2019;81:2474-2488.

8. Gunther M, Bock M, Schad LR. Arterial spin labeling in combination with a look-locker sampling strategy: inflow turbo-sampling EPI-FAIR (ITS-FAIR). *Magn Reson Med*. 2001;46:974-984.

9. Varela M, Petersen ET, Golay X, Hajnal JV. Cerebral blood flow measurements in infants using Look-Locker arterial spin labeling. *J Magn Reson Imaging*. 2015;41:1591-1600.

10. Gunther M. Encoded continuous arterial spin labeling. In: Proceedings of the ISMRM Workshop on Cerebral Perfusion and Brain Function: Novel Techniques and Applications, Salvador, Bahia, 2007.

11. Wells JA, Lythgoe MF, Gadian DG, Ordidge RJ, Thomas DL. In vivo Hadamard encoded continuous arterial spin labeling (H-CASL). *Magn Reson Med*. 2010;63:1111-1118.

12. Dai W, Shankaranarayanan A, Alsop DC. Volumetric measurement of perfusion and arterial transit delay using Hadamard encoded continuous arterial spin labeling. *Magn Reson Med*. 2013;69:1014-1022.

13. Teeuwisse WM, Schmid S, Ghariq E, Veer IM, Van Osch MJP. Time-encoded pseudocontinuous arterial spin labeling: basic properties and timing strategies for human applications. *Magn Reson Med*. 2014;72:1712-1722.

14. Parker DL, Goodrich KC, Roberts JA, et al. The need for phase-encoding flow compensation in high-resolution intracranial magnetic resonance angiography. *J Magn Reson Imaging*. 2003;18:121-127.

15. Hennig J, Nauerth A, Friedburg H. RARE imaging: a fast imaging method for clinical MR. *Magn Reson Med*. 1986;3:823-833.

16. Chappell MA, Groves AR, Whitcher B, Woolrich MW. Variational Bayesian inference for a nonlinear forward model. *IEEE Trans Signal Process*. 2009;57:223-236.

17. Groves AR, Chappell MA, Woolrich MW. Combined spatial and non-spatial prior for inference on MRI time-series. *Neuroimage*. 2009;45:795-809.

18. Elsayed M, Sammani F, Hamdi A, Al-Baser A, Babalghoom H. A new method for full reference image blur measure. *Int J Simul Syst Sci Technol*. 2018;19:4.

19. R Core Team. *R: A Language and Environment for Statistical Computing. Foundation for Statistical Computing*. Vienna, Austria: R Foundation for Statistical Computing; 2020. https://www.R-project.org/. Accessed March 12, 2021.

20. Vidorreta M, Wang Z, Rodriguez I, Pastor MA, Detre JA, Fernández-Seara MA. Comparison of 2D and 3D single-shot ASL perfusion fMRI sequences. *Neuroimage*. 2013;66:662-671.

21. Wang J, Alsop DC, Song HK, et al. Arterial transit time imaging with flow encoding arterial spin tagging (FEAST). *Magn Reson Med*. 2003;50:599-607.

22. Le TT, Fischbein NJ, André JB, Wijman C, Rosenberg J, Zaharchuk G. Identification of venous signal on arterial spin labeling improves diagnosis of dural arteriovenous fistulas and small arteriovenous malformations. *Am J Neuroradiol*. 2012;33:61-68.

23. Wolf RL, Wang J, Detre JA, Zager EL, Hurst RW. Arteriovenous shunt visualization in arteriovenous malformations with arterial spin-labeling MR imaging. *Am J Neuroradiol*. 2008;29:681-687.

24. van Osch MJP, Teeuwisse WM, Chen Z, Suzuki Y, Helle M, Schmid S. Advances in arterial spin labelling MRI methods for measuring perfusion and collateral flow. *J Cereb Blood Flow Metab*. 2018;38:1461-1480.

25. Chappell MA, MacIntosh BJ, Donahue MJ, Günther M, Jezzard P, Woolrich MW. Separation of macrovascular signal in multi-inversion time arterial spin labelling MRI. *Magn Reson Med*. 2010;63:1357-1365.

SUPPORTING INFORMATION

Additional Supporting Information may be found online in the Supporting Information section.

FIGURE S1 Two representative slices for all postlabeling delays (PLDs) and readout schemes in sagittal view

FIGURE S2 A, Arterial blood volume (aBV) maps quantified from the time-encoded pseudo-continuous arterial spin labeling (pCASL) data in a representative subject. Color bar shows aBV range in mL/100 g. B, The aBV maps quantified from the time-encoded pCASL data for each different flow compensation (FC) level. Color bar shows aBV range in mL/100 g

FIGURE S3 A, Cerebral blood flow (CBF) maps quantified from the time-encoded pCASL data in a representative subject for the different readouts. Color bar shows CBF range in mL/100 g/min. B, The CBF maps quantified from the time-encoded pCASL data for each different FC level. Color bar shows the CBF range in mL/100 g

FIGURE S4 Two representative slices for all PLDs and each FC level acquired